WatAIR: A Fluidized-Bed, Moisture-Swing Adsorbent, and Algae-Based Utilization Approach to CDR

Robert Duff
Department of Chemical Engineering
University of Waterloo
Waterloo, ON, Canada
rduff@uwaterloo.ca

***Abstract*—This paper describes the development of a carbon capture and utilization prototype system, employing a novel phosphate-activated moisture-swing adsorbent in a fluidized bed reactor configuration and the utilization capabilities of algae (*C. vulgaris*). This application of a fluidized bed reactor combined with the resin-PO4 IRA-900 moisture-swing adsorbent developed, is the first-of-its-kind according to best available information In previous versions of the prototype, due to limitations in CO_2 sensing equipment and sorbent drying methods, the capture performance of the system was not able to be determined. In this design, correcting for these limitations, the capture performance was able to be validated and peak adsorption rates were determined to be approximately 0.95 g mol^{-1} h^{-1}. The moisture content of the sorbent after each adsorption and desorption cycle was measured to be on average 6.72% and 59.54%, respectively. As the sorbent was measured to lose over 80% of its water content, the heated environment was concluded to be sufficient for ensuring near maximum dehydration. Algal growth and CO_2 fixation analyses were performed before improvements in sorbent drying, resulting in apparent but minimal growth in *C. vulgaris* from an optical density of 1.65 to 1.8 OD. This report also details investigations into alternative reactor designs and components for future consideration and development.**

I. Introduction

As the atmospheric concentration of carbon dioxide (CO_2) continues to increase, the capability of natural carbon cycle and the currently planned emissions reduction strategies are proving increasingly insufficient for mitigating climate change. Among many environmental scientists, professionals, and research institutions, it is well understood that in order to meet emissions targets designed to avoid the worst impacts of climate change, carbon dioxide removal (CDR) is a critical piece of the multifaceted solution required. Many environmental professionals and institutions agree that to mitigate climate change to a manageable degree, some form of carbon dioxide removal (CDR) is required [10]. In response to a 2015 National Academies report, Climate Intervention: Carbon Dioxide Removal and Reliable Sequestration, the National Academies published a report in 2019 which found that, to meet established climate goals, approximately 10 Gt/yr of removal would be needed by mid-century, increasing to 20 Gt/yr by the end of the century [3]. The field of CDR is comprised of a diverse range of technologies and unique approaches, each with their own challenges and limitations. This 2019 report focused on the four most prominent land-based approaches ready for large-scale deployment: afforestation/reforestation, changes in forest management, uptake and storage by agricultural soils, and bioenergy with carbon capture and storage. The study considered these approaches based on their potential for CDR at costs of \$100/tCO_2 or less however, doesn't consider non-land approaches like ocean-based CDR and direct air capture (DAC) [10].

Although the field of ocean-based CDR shows promise, with research underway by a variety of institutions including Ocean Networks Canada with their Solid Carbon project off the coast of Vancouver Island, direct air capture technology has developed significantly in recent years and is the focus of this investigation. This paper describes the exploration, design, and testing of a novel prototype system that employs a method of DAC known as moisture-swing adsorption (MSA). The novelty of the system lies in the unique adsorbent preparation method and application of a MSA adsorbent in a fluidized bed system. While biological CO_2 sequestration/utilization is not new, the use of microalgae for this purpose strengthens the novelty of the prototype system, showcasing its advantages for moisture swing adsorption.

II. Background

A. Common Mechanisms of DAC

The field of DAC has advanced rapidly in part due to developments with solid sorbents, which have been applied widely in carbon capture and sequestration (CCS) projects worldwide. Adsorbents typically operate on one of two methods of adsorption: physisorption and chemisorption. In physisorption, the adsorbate – such as CO_2 – adheres to the adsorbent surface due to weak intermolecular forces without forming chemical bonds. In chemisorption, however, the adsorbate forms a chemical bond with active ions on the adsorbent surface. To desorb the component, energy is required to reverse

the reactions binding the CO_2, which is typically around 45-50 kJ/mol [14]. This process of adsorption and desorption is commonly referred to as swing adsorption.

Although this investigation is centered around MSA, there are three recognized typical swing adsorption processes; Pressure Swing Adsorption (PSA); Temperature Swing Adsorption (TSA); and Vacuum Swing Adsorption (VSA). In PSA processes, the system operates at a high pressure until saturation, at which the system pressure is lowered, and the sorbent is regenerated. The process for VSA systems is like that of PSA although applying a vacuum allows the system to operate at a lower starting pressure. For TSA, this involves superheating the catalyst along with pressure swings to supply enough energy in the form of heat to force the reverse reaction of CO_2 and the sorbent surface [16].

While each process has its own advantages, factors of energy consumption, target gas production, and regeneration ability determine the appropriate application of each process. Typically, non-MSA processes utilize a zeolite catalyst to perform the desired reaction mechanisms. For CDR, these zeolites are specially prepared to increase their reactivity with CO_2 as well as to match the operational properties of their swing systems [18]. They are typically arranged in a vessel or bed where a feed gas is channelled through, removing the impurities or desired compounds from the feed stream. Once the zeolite catalyst is saturated, reaching their maximum capture capacity, they are regenerated to release the captured compound allowing the zeolite to be reused.

B. Moisture Swing Adsorption (MSA) for CDR

Moisture Swing Adsorption (MSA) has recently been proposed for CO_2 capture from air, particularly as a solution for addressing small and distributed source emissions as current carbon capture and sequestration techniques are designed to treat primarily large point sources [17]. Unlike other adsorption processes, MSA eliminates the need for heat or pressure changes to drive the adsorption/desorption cycle, instead relying on water. Its evaporation provides the free energy required to drive the process. MSA aims to address issues with typical processes such as energy usage, safety, and system complexity/cost. As it doesn't require high temperatures or complex pressure control systems, energy requirements can be significantly reduced. This also reduces the emissions impact of operating the system assuming energy is supplied by carbon emitting sources.

The mechanism of MSA chosen for this system is chemisorption on the amine-functionalized polymeric sorbent Amberlite™ IRA-900. As an anion exchange membrane, positively charged functional groups on the sorbent surface attract and bind with the adsorbent, displacing other anions on the sorbent's structure. The capture capacity of the sorbent is thus dependent on the specific functional group and subsequent reaction mechanism, as well as level of hydration for MSA sorbents [17]. Research suggests that multivalent anions are the most promising for moisture swing applications. There are valuable opportunities to engineer the sorbents since the anions in a sorbent's resin matrix can be modified or replaced, thus offering the potential to increase CO_2 selectivity.

In 2011, Wang et al. proposed an amine-based anion exchange resin, with quaternary ammonium cation functional groups, co-extruded with polypropylene as a flat sheet. This sorbent, whose original exchangeable anions are chloride ions, incapable of CO_2 adsorption, would require further treatment with alkaline solutions to replace the exchangeable anion with hydroxide or carbonate ions. Once replaced, during adsorption, the exchangeable ions would follow the reaction mechanisms visualized in Figure 1 for the respective adsorption and desorption steps [17].

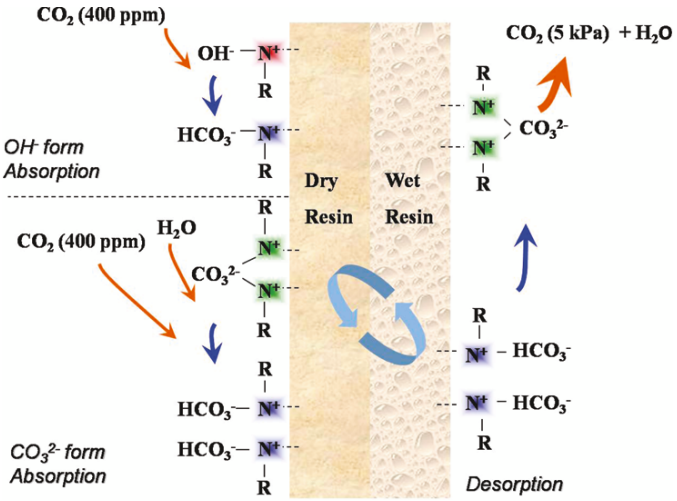

Fig. 1. Visualization of adsorption mechanisms on MSA adsorbents with OH^- and CO_3^{2-} form functional groups [17].

Generalized for a generic ion "R" with ionic charge "q", the specific reaction mechanisms that define the adsorption process can be defined by the following equations. Equation 3 depicts the overall adsorptive reaction as a combination between the active ion interactions defined by Eq. 1 which generate OH^- ions required by Eq. 2 for CO_2 binding. In these relationships, "n" is the degree of ionic hydration and m_1, m_2, and m_3 are the coefficients of the water molecules consumed and produced in the reactions,

$$\mathrm{R}^q \cdot n\mathrm{H_2O} \rightleftharpoons \mathrm{HR}^{q+1} \cdot m_1\mathrm{H_2O} + \mathrm{OH}^- \cdot m_2\mathrm{H_2O} + (n-1-m_1-m_2)\mathrm{H_2O} \quad (1)$$

$$\mathrm{OH}^- \cdot m_2\mathrm{H_2O} + \mathrm{CO_2} \rightleftharpoons \mathrm{HCO_3}^- \cdot m_3\mathrm{H_2O} + (m_2-m_3)\mathrm{H_2O} \quad (2)$$

$$\mathrm{R}^q \cdot n\mathrm{H_2O} + \mathrm{CO_2} \rightleftharpoons \mathrm{HR}^{q+1} \cdot m_1\mathrm{H_2O} + \mathrm{HCO_3}^- \cdot m_3\mathrm{H_2O} + (n-1-m_1-m_3)\mathrm{H_2O} \quad (3)$$

C. Microalgal CO_2 Fixation

While traditional sequestration techniques aim to synthetically store or convert CO_2, such as geological or oceanic storage and electrochemical conversion, biological conversion

is, on average, a simpler method that yields several advantages and ancillary benefits. Biological conversion is a promising option due to is economic and technological viability, which are both key areas of challenge and shortfall for most sequestration methods. For example, electrochemical conversion is only economically feasible in select countries, and the transportation of captured carbon poses logistical complexities, costs, and possibilities of CO_2 leakage [12]. While these limitations also exist for biological sequestration/utilization, their magnitude is much less in comparison.

Although the operation and maintenance of a large-scale closed photo-bioreactor has a high cost, and alternatives like open-raceway ponds show low conversion efficiency, biological sequestration/utilization is becoming a more popularly investigated solution [20]. The primary reasoning for the increasing research into this solution is that microalgae can transform atmospheric CO_2 into plant biomass with higher photosynthetic efficiency than most terrestrial plants, it does not occupy arable land, it uses cheap nutrient feedstocks (e.g. wastewater), and as an end-stage benefit, the economic value of the biomass produced can help offset its production costs [12]. Specific strains such as *C. vulgaris* which has been cultured in the system prototype, have a well-documented ability to adapt to extreme environmental conditions.

C. vulgaris as a strain is a single-celled organism that can survive in temperate and tropical environments, sourcing nutrients from soil to hot springs, while the recovery of a closely related strain from polar regions also suggests a tolerance for lower temperatures [8]. This resilience makes it well suited for incorporation into an open-source CDR system. Under unfavourable environmental conditions, researchers at the University of Waterloo, such as Dr. Valerie Ward, have further cited that *C. vulgaris* can live up to 6 months in the stationary phase (equal cell growth/death).

III. Prototype System Novelty

A. Phosphate Activated Ion Exchange Resin IRA-900

Traditionally, as visualized by Figure 1, MSA adsorbents operate through hydroxide-form (OH–) or carbonate-form (CO_3^{2-}) adsorption. However, a study published in 2019 proposed a phosphate-activated resin sorbent which reported an 80% increase in adsorption capacity compared to CO_3^{2-} form. The sorbent, developed through treatment of D201 macroporous ion-exchange resin (IER) with potassium phosphate tribasic, also showed higher adsorption rates within a temperature range of 15–35 °C [15]. Supporting these conclusions, in comparison to the fifteen other molecules tested, Hegarty et al. showed that the phosphate divalent co-ion has a higher mass-normalized CO_2 moisture-swing capacity [7]. Based on this study, the adsorbent used in this investigation underwent pre-treatment to introduce dibasic phosphate anions into its resin matrix. As resin-PO4 sorbents have been studied before, the novelty of this pre-treatment arises from the materials used. Specifically, as opposed to D201 IER, the system used IRA-900 pursuant to research by Liu et al. (2024), which showed that while the capture capacity was not the greatest of the materials studied, it had the greatest capture capacity stability of 100% after 100 cycles [9]. Coupled with the results of Hegarty et al. (2023), treating the sorbent with sodium phosphate dibasic, we developed a new humidity swing absorbent based on PO_4^{3-}/HPO_4^{2-}/$H_2PO_4^{-}$ ions, with IRA-900 as the IER backbone [7].

B. Reactor Design

As the WatAIR team operates as a portfolio of the Engineers Without Borders UWaterloo Chapter (UW EWB), the prototype was created to align with UW EWB's core values, with a specific focus on equal and open access relating to engineering development. As such, the WatAIR carbon removal system was developed for the purpose of making CO_2 removal accessible to the public with a total system cost of under $2000. Apart from technical equipment such as pumps, valves, sensors, and certain fittings, custom 3D printed parts were designed and applied wherever feasible. The system was designed to be entirely automated with a control sequence and data monitoring system using the open-source Arduino and Raspberry Pi ecosystems, comprised of 15 Arduino-controlled relays controlling every aspect of the process. To promote accessibility, all the equipment and sensors used are readily available, low cost, and open source.

IV. Materials and Methods

A. Material Process and Characterization

Pretreatment. The material (Amberlite^{TM} IRA-900 Cl^-) tested was supplied by Sigma-Aldrich (St. Louis, MO, USA) and was originally intended for use in industrial water treatment applications. For the material to absorb CO_2, the original exchangeable chloride ions were replaced with phosphate ions, introduced by washing the resin particles in a phosphate solution. The resin particles were first washed and soaked in deionized (DI) water, at 85–95°C for 48 hours, to induce swelling in the resin to open the matrix structure sufficiently for anion replacement. The material was washed using a 0.5 M sodium phosphate dibasic solution for 2-4 hours and stirred to enhance the ion exchange. After every wash, the material was rinsed with DI water, collecting solution and wash residual for titration. The material was washed and rinsed 6-7 times until no chloride was detected in the solution by titration.

Resin Characterization. The material pre-treatment procedure was validated by chloride salt titration of the solution and wash residuals. The full procedure can be found in the Supplementary Materials. The sixth and seventh washes were determined to have chloride concentrations of 0.44 M and 0.33 M respectively, indicating that chloride displacement was successful although not entirely evidenced by the remaining chloride in the final wash. Due to the porous structure of the IER, the treated IRA-900 has a surface area between 16.01 m^2/g and 17.14 m^2/g (Gemini VII BET Surface Area Analyzer, Micromeritics), analyzed in triplicates for two individually treated samples. This treatment method and application of the sorbent in bead form should theoretically result in a higher capacity for CO_2 adsorption as opposed to the 2 m^2/g

surface area of the polymerized extrusion proposed by Wang et al. [17].

V. Overview of Process and Final Prototype

A. General Operating Mechanism

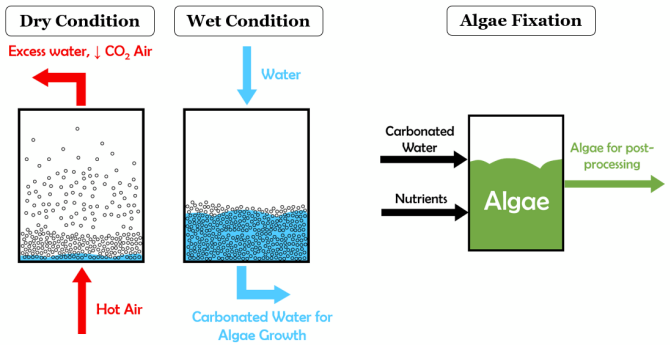

Fig. 2. Three step, cyclic operating process of the WatAIR prototype.

Over a standard 2-hour run, the prototype operates in a three-step sequential process visualized in Figure 2. The first stage is referred to as the dry condition and involves the flow of ambient air through the base of the column containing the treated IER sorbent beads on which CO_2 is adsorbed. During this stage, the flowing air as well as the low particle density creates a fluid-like behaviour in the sorbent particles, characteristic of fluidized beds, and is utilized to increase available contact area for gas-solid interactions and capture. Once the sorbent is saturated, measured through breakthrough analysis of the air leaving the column, the system switches to stage two: the wet condition. In this stage, DI water is misted through the column until the IER is fully hydrated, approximately five minutes, and allowed to stand for an equal amount of time to allow the sorbent to desorb. The process water is then passed to the final stage where its stored and automatically pumped to an algae bioreactor, along with required growth nutrients, depending on algae density.

Fig. 3. IRA-900 sorbent (A) before wetting and (B) after wetting.

The dry and wet conditions operate cyclically, using the air flow after the wet condition to simultaneously dehydrate the sorbent particles and re-initiate capture. The dehydration process is aided by a 1500 W heating cable, supplied by McMaster-Carr (Elmhurst, IL), wrapped around the column to ensure a uniform temperature not exceeding 50°C to avoid material degradation at higher temperatures. One indicator of sufficient drying is the swelling effect when the particles are exposed to water, shown in Figure 3. A visual demonstration of these stages in operation can be found in the Supplementary Materials.

B. Prototype Setup and Components

The prototype construction is separated into four levels of components, as shown in Figure 3 and Table 1. The first and top-most level contains components relating to the adsorption and desorption steps of the process. The primary component in this level is the column in which the sorbent is housed, with a series of valves and water pumps as secondary components. The column is composed of a borosilicate glass tube with metal flanges and supports at each end, sitting on a custom polyethylene terephthalate glycol (PETG) stand for air supply and water drainage. To prevent material loss, a stainless steel 100-mesh screen is placed at the base of the column with a hydrophobic polyethylene (PET) sheet (1/16" Hydrophobic Large Pore Size Sheet, POREX) at the other end. Although the 100-mesh screen prevented material loss and accumulation, it was also found to degrade the material due to constant collisions during fluidization. The PET sheet's hydrophobic attributes were originally introduced to address the limitation of NDIR CO_2 sensors misinterpreting water droplets for CO_2 due to similar infrared spectra. These sheets now serve as an additional waterproofing measure to protect the enclosed Telaire T6615-F CO_2 sensor which reads the exiting air, pumped at a rate of 0.5 liters per minute, at 5 s intervals.

During the wet condition, DI water supplied by a 45 W pump is evenly distributed at a rate of 1.6 mL/s with approximately 250 mL collected every cycle. The carbonated water is stored in an airtight tank before being fed in controlled intervals to the microalgae bioreactor. In the bioreactor, dissolved CO_2 in the form of bicarbonate ions serve as an inorganic carbon source for the microalgae. Automated, the system maintains a fluid volume in the bioreactor of 3.6 L, which is 70% of its 5.2 L capacity, for safety purposes, and an average algal concentration of 0.26 g/L. Using a series of turbidity and level sensors, the system automatically pumps algae from the reactor to external storage once the concentration exceeds 2.6 g/L and adjusts the fluids and nutrients, maintaining the operating volume. A visual demonstration of the CO_2 fixation process can be found in the Supplementary Materials.

VI. Monitoring, Reporting, and Verification (MRV)

A. CO_2 Capture Performance

Limitations of our previous design iterations with respect to the MRV of capture performance revolved around two

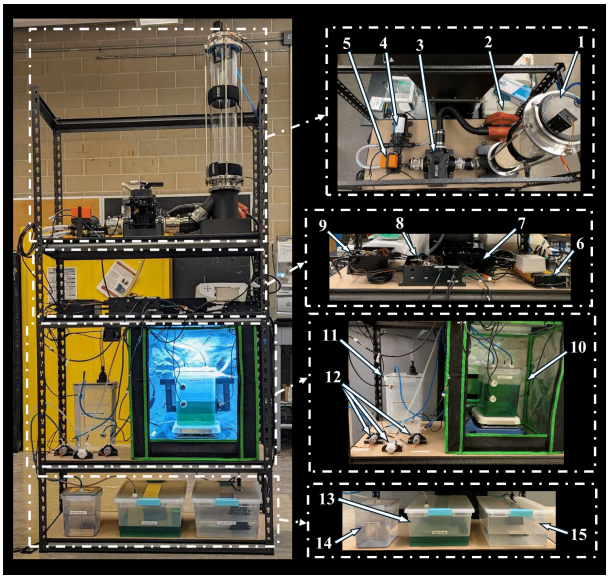

Fig. 4. Prototype system with numbered components, identified in Table II.

TABLE I
PROTOTYPE SYSTEM COMPONENT LABELS FOR FIGURE 4

ID	Description	ID	Description
1	Column with resin sorbent	9	DC circuit control
2	Leaf blower	10	Algae growth reactor
3	3-way Jandy valve	11	Carbonated water storage
4	Water pump	12	Peristaltic pumps
5	2-way brass ball valve	13	Excess algae storage
6	Power bar	14	Algae nutrient storage
7	AC circuit control	15	DI water supply
8	Sensor control		

issues: CO_2 sensing equipment and sorbent drying. One of the primary technologies used for CO_2 in air detection is NDIR or non-dispersive infrared, which determines gas concentrations by passing infrared light through a sample and filtering the detected light based on the characteristic absorption spectra [13]. As NDIR sensors are dependent on the comparison between readings and characteristic absorption spectra, humidity has been shown to influence the accuracy of readings. This is partly because of specific similarities between emission bands of CO_2 and H_2O, shown in Figure 5, where they both share peaks at a wavelength around 2.5 microns. When exposed to high humidity samples, the low-cost nature of these sensors may result in misinterpretation of H_2O in air for CO_2, inflating readings. This was evident in our results with the SCD-41 where peaks in CO_2 concentration directly correspond with peaks in humidity, shown in Figure 6. As well, the SCD-41 was determined to be incompatible with flowing air, contributing further inaccuracies, considering the fluidized bed air flow design.

To resolve the issue of humidity spikes causing false peaks in CO_2 concentration, as opposed to the 100-mesh stainless steel filter used at the base of the column, a hydrophobic

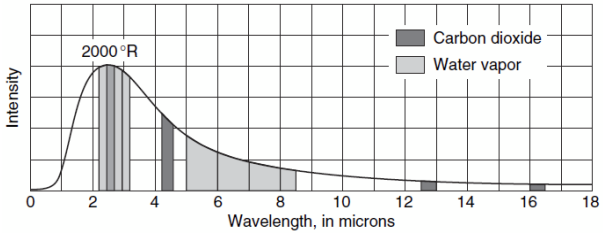

Fig. 5. Emission bands of CO_2 and H_2O [19].

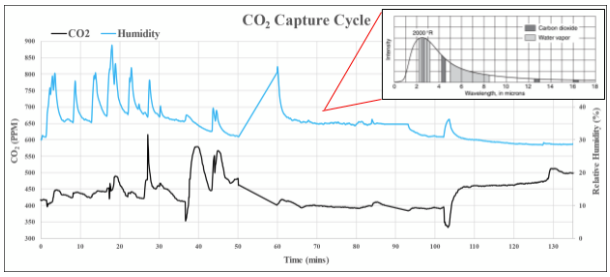

Fig. 6. Dependence of outlet CO_2 concentration measurement on humidity overlayed with CO_2 and H_2O IR spectra [19].

PET sheet was used to prevent as much liquid water from being expelled from the column which resulted in no observed CO_2 spikes in experimental results. By also replacing the SCD-41 sensor with the Telaire T6615-F, an NDIR sensor specifically designed for flowing air up to 0.5 lpm, the readings became more normalized and ranged within reasonable values for ambient air. The result of these changes can be seen by experimental runs where distinct breakthrough curves were identified and fitted with a sigmoid curve in Figure 7. Assuming an air velocity of 2.5 m/s through the 3" diameter column, measured by anemometer, and integration above the curve prior to saturation, the peak adsorption rates were determined to be approximately 0.78 and 0.95 g mol^{-1} h^{-1} for Run A and Run B, respectively. These results appear consistent with those published by Liu et al., whose formulation yielded a peak adsorption rate of 1.28 g mol^{-1} h^{-1}.

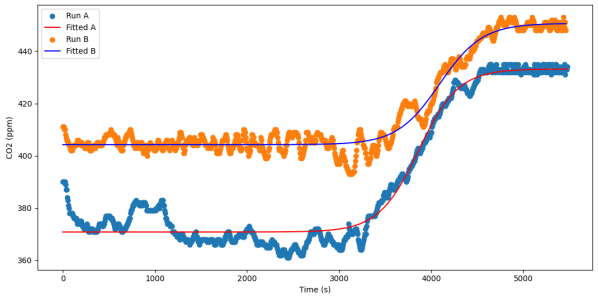

Fig. 7. CO_2 concentration in exiting air of the prototype, fitted with a sigmoid curve to show breakthrough.

The second limitation was sorbent moisture content, specifically ensuring effective drying over the course of the capture cycle. As reported by Wang et al., for IRA-900 to achieve

full saturation, a relative humidity of less than 1% is required while previous methods of this prototype had only been able to achieve 30%. While moisture swing adsorption is low-cost and shows minimal capacity to degrade the material during desorption, the relationship between moisture content and capture capacity is a significant disadvantage. In the past, we theorized that residual moisture was a likely perpetrator for our limited capture capacity and lack of distinct breakthrough analysis. By applying industrial heating wrap around the column, maintaining a consistent environmental temperature of around 50 °C, the sorbent has an average moisture content of 6.72% after each dry condition, compared to 59.54% after each wet condition.

B. CO_2 Conversion Performance

While the exact amount of CO_2 "fixed" by microalgae has been difficult to determine, there are several methods we have employed to verify its progress. The first method is measuring the captured CO_2 in the process waters, initially through the development of a custom dissolved CO_2 sensor detailed in the Supplementary Materials. Additionally, pH analysis of the process water compared to bottled carbonated water was employed to measure fixation/growth. Through periodic analysis over four days, the change in pH of both sample waters was observed. From these results, shown in Figure 8, it was observed that both samples equilibrate around 7-8 pH within 24 hrs, with the process water beginning at a pH of around 7.03 and the bottled beginning at a pH of around 5.4. The process water began with a lower pH than the DI supplied to the column (7.3), suggesting dissolution of captured CO_2, that is the reduction of pH of a solution due to its dissociation reaction mechanisms according to the carbon cycle. In the absence of a dissolved CO_2 sensor, this is a positive indicator of CO_2 desorption efficiency.

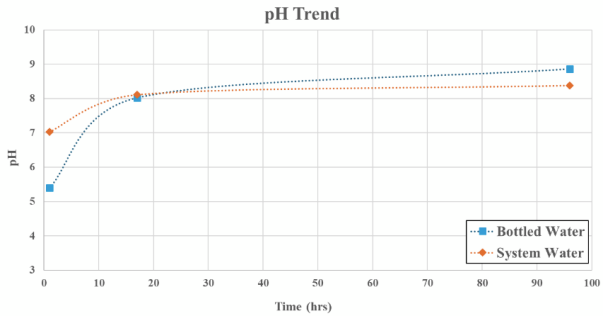

Fig. 8. pH of process water and bottled carbonated water samples over four days.

Another method of verification used was the study of growth performance of *C. vulgaris* microalgae using process water and bottled carbonated water as inorganic carbon sources. The results, presented in Figure 9, showed some growth compared to the bottled carbonated water due to a change in optical density from 1.65 to 1.8 OD. However, the process water did not depict exponential growth like the bottled water did. It should be noted that the initial drop in OD around 70 hours for the bottled water was due to random or human error. This study was conducted prior to the addition of the heating system using a 20 mL bioreactor (Pioreactor 20ml v1.1, Pioreactor) with a stir rate, regulated temperature, and light intensity of 500 rpm, 25°C, and 100 µmol m^{-2} s^{-1}, reading optical density in five second intervals. These results seem consistent with the assumptions made that due to insufficient drying, the sorbent capture capacity was minimized and thus the amount of desorbed CO_2 was assumed to have been insufficient for exponential growth. It is also possible that the chemical properties of IRA-900 influence the system water in such a way that inhibits algal growth although further chemical and biological analysis, outside of the scope of this project, would be required to confirm this hypothesis.

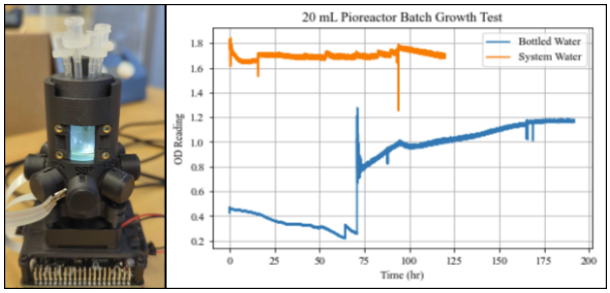

Fig. 9. Pioreactor setup (left) and optical density of algae in both system and bottled water samples over 8 days (right).

Additional tests need to be completed to achieve reproducible growth curves where the exponential growth phase is observed. Once growth is reproducibly studied, cycle times for the system can be determined, a documented rate of 0.26g/l/d is expected [20].

C. Life Cycle Assessment

Power consumption. Per adsorption and desorption cycle, approximately 0.484 kWh of energy is used to power the equipment which translates to an average of 14.4 gCO_2 in an 85-minute cycle assuming energy is supplied by the Ontario power grid [11]. The emitted CO_2 was determined by taking the sum of the power requirements of each individual component over their respective duration of use in each cycle and then applying the Ontario grid emission factor.

Material consumption. The scope of this analysis was limited to major devices with relatively publicly available material breakdowns while the emissions from factors like consumables such as gloves and fasteners were not included. The analysis concluded that the system has a single-point emission of 130 gCO_2 for its construction.

VII. Potential for Future Development

The focus for future development of WatAIR's design is circularity and development of low-cost open-source resources. This will include researching sustainable algae feedstock and developing reliable CO_2 sensing devices. To improve the efficacy of the current design, mechanisms to further reduce water vapor concentrations are being explored. Longer sorbent

drying cycles and the application of mechanical pressure are options being studied for more effective sorbent drying.

A partnership has been established with the low-cost, open-source bioreactor start-up based in Waterloo, Canada. Their product, "Pioreactor", was used to perform our algae growth batch tests. Over the past year, and continuing into the future, our team received sponsorship from the start-up to aid with the development of a dissolved CO_2 sensor compatible with the Pioreactor ecosystem. For our team, the development of this sensor be more economically viable than purchasing one that's commercially available and it will also improve accessibility into the CO_2 removal space.

The current photobioreactor design can also be improved to enhance algae growth. One study of Chlorella Vulgaris growth found high growth yields using an airlift photobioreactor. Flat-type, open thin-layer, and normal vertical tubular photobioreactors are alternate bioreactor options utilized in carbon capture applications [2]. Increased algae growth resulting from an improved photobioreactor model will allow for increased use of microalgae in different markets. Market studies for microalgae, specifically C. Vulgaris, applications and demand is required to further establish the target end-use of its cultivation via carbon capture and further enhance the circularity of the design.

A. Alternative Reactor Configurations and Additional Components

Fig. 10. Designs and components for future development: (A) Three column reactor design, (B) heating element enclosure, and (C) open-source orbital shaker.

To address the issues of sorbent drying and low capture capacity observed in previous iterations of the prototype, a new reactor configuration was proposed and investigated. The alternative design features a three-column setup composed of acrylic tubing for the columns with fully 3D printed flanges, tubing, and platform. This design aims to increase the replicability and accessibility of our prototype by replacing costly glass and metal components with materials that could be made by anyone with access to the increasingly widespread 3D printing technology.

By separating the system into three columns as opposed to one, ideally the extend of sorbent drying per cycle would increase with less sorbent in each column, maintaining the total amount of sorbent used. Depending on the results, the amount of sorbent could be gradually increased to increase the capture capacity of the system while ensuring that the increase wouldn't significantly impact drying extent. During testing, the three column structure was durable, lightweight, and provided a good seal which minimized sorbent loss during operation. However, the largest issue with this design was ensuring equal air flow between all three columns. Despite various designs and iterations, the air supply always favoured one or more columns leading to low or no flow in others. In the interest of time and producing actionable results, we reverted to a single borosilicate column design. As a secondary solution, a custom enclosure printed out of acrylonitrile butadiene styrene (ABS) to house the heating mechanism of a standard hair dryer. The enclosure could then be placed in the air flow line to add additional heat to the system and accelerate drying. The heating tape was found to dry the sorbent sufficiently and thus, the enclosure was not applied in the final prototype.

To properly agitate the algae during fixation without the use of a physical stirring mechanism that may damage the microalgae, an open-source orbital shaker (DIYbio Orbital Shaker V 2.0, ProgressTH) was printed and integrated into the system. The shaker was low-cost, required little power, and agitated algal samples sufficiently to prevent accumulation and enable growth. Although some conclusions have been made, these three designs/components will be further investigated and developed to their fullest extent.

Finally, in partnership with the Pioreactor company, a custom small-scale dissolved CO_2 sensor will continue to be developed. The dissolved CO_2 (dCO_2) meter operates on the basis of gas diffusion through a semi-permeable membrane within a closed loop system using low-cost and small-scale components. Initially designed with custom 3D printed UV resin enclosures to house an SCD-41 CO_2 sensor, future versions will be looking at replacing the sensor with a sensor capable of maintaining a vacuum, required by the design in order to ensure gas purity within the sample loop. A rough render of the first prototype of the dCO_2 meter is shown in Figure 11.

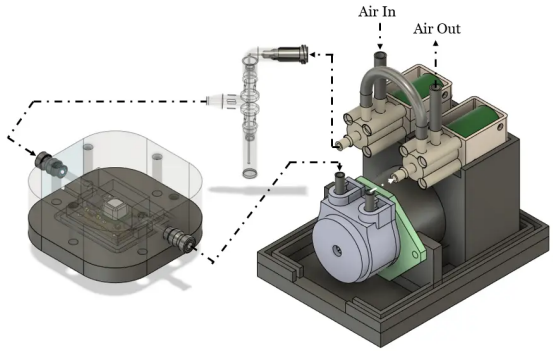

Fig. 11. Render of the Pioreactor dCO_2 meter version 1.0.

ACKNOWLEDGEMENTS

The author would like to thank Dr. XiaoYu Wu for his outstanding support and guidance of the team as Project

Advisor since its inception as well as Katherine Nguyen and Laurel Pierroz-Wong for their support in the development of the prototype and this report.

Many thanks as well to David Lang and the representatives of the Experiment Foundation for their financial support of this project through the Negative Emissions Technology Challenge Grant, awarded to our project titled "Low-Cost, Open-Source Carbon Capture and Utilization System" on the Experiment.com platform.

Finally, many thanks to all those who volunteered their time and expertise to this project including:

- Dr. Valerie Ward and Reza Roushan
- Peter Teertstra and Graeme Adair from the Sedra Student Design Center at the University of Waterloo
- Krysta Traianovski and Matthew Noble from Velocity Science
- Engineers Without Borders Waterloo Chapter

References

[1] Pahola Thathiana Benavides, Uisung Lee, and Omid Zarè-Mehrjerdi. "Life cycle greenhouse gas emissions and energy use of polylactic acid, bio-derived polyethylene, and fossil-derived polyethylene". In: *Journal of Cleaner Production* 277 (Dec. 2020), p. 124010. ISSN: 09596526. DOI: 10.1016/j.jclepro.2020.124010. URL: https://linkinghub.elsevier.com/retrieve/pii/S0959652620340555 (visited on 03/10/2025).

[2] Viki R. Chopda et al. "Real-time dissolved carbon dioxide monitoring I: Application of a novel in situ sensor for CO_2 monitoring and control". In: *Biotechnology and Bioengineering* 117.4 (Apr. 2020), pp. 981–991. ISSN: 0006-3592, 1097-0290. DOI: 10.1002/bit.27253. URL: https://onlinelibrary.wiley.com/doi/10.1002/bit.27253 (visited on 03/09/2025).

[3] Committee on Developing a Research Agenda for Carbon Dioxide Removal and Reliable Sequestration et al. *Negative Emissions Technologies and Reliable Sequestration: A Research Agenda*. Pages: 25259. Washington, D.C.: National Academies Press, Mar. 8, 2019. ISBN: 978-0-309-48452-7. DOI: 10.17226/25259. URL: https://www.nap.edu/catalog/25259 (visited on 03/09/2025).

[4] *Emission factors in kg CO2-equivalent per unit*. City of Winnepeg. URL: https://www.winnipeg.ca/finance/findata/matmgt/documents/2012/682-2012/682-2012_Appendix_H-WSTP_South_End_Plant_Process_Selection_Report/Appendix%207.pdf?utm_source=chatgpt.com.

[5] G. Poszmik, HS Kim, and J Choo. *Estimating the Impact of Using Recycled PTFE on CO2 Emissions*. Shamrock Technologies Inc. URL: https://shamrocktechnologies.com/co2-emissions/..

[6] Rita Garcia and Fausto Freire. "Carbon footprint of particleboard: a comparison between ISO/TS 14067, GHG Protocol, PAS 2050 and Climate Declaration". In: *Journal of Cleaner Production* 66 (Mar. 2014), pp. 199–209. ISSN: 09596526. DOI: 10.1016/j.jclepro.2013.11.073. URL: https://linkinghub.elsevier.com/retrieve/pii/S0959652613008494 (visited on 03/10/2025).

[7] John Hegarty et al. "Expanding the Library of Ions for Moisture-Swing Carbon Capture". In: *Environmental Science & Technology* 57.50 (Dec. 19, 2023), pp. 21080–21091. ISSN: 0013-936X, 1520-5851. DOI: 10.1021/acs.est.3c02543. URL: https://pubs.acs.org/doi/10.1021/acs.est.3c02543 (visited on 03/08/2025).

[8] Ladislav Hodač et al. "Widespread green algae *Chlorella* and *Stichococcus* exhibit polar-temperate and tropical-temperate biogeography". In: *FEMS Microbiology Ecology* 92.8 (Aug. 2016). Ed. by Rosa Margesin, fiw122. ISSN: 1574-6941. DOI: 10.1093/femsec/fiw122. URL: https://academic.oup.com/femsec/article-lookup/doi/10.1093/femsec/fiw122 (visited on 03/09/2025).

[9] Shuohan Liu et al. "Robust Enhancement of Direct Air Capture of CO2 Efficiency Using Micro-Sized An-

ion Exchange Resin Particles". In: *Sustainability* 16.9 (Apr. 25, 2024), p. 3601. ISSN: 2071-1050. DOI: 10.3390/su16093601. URL: https://www.mdpi.com/2071-1050/16/9/3601 (visited on 03/08/2025).

[10] National Academies of Sciences, Engineering, and Medicine (U.S.), ed. *A Research Strategy for Ocean-Based Carbon Dioxide Removal and Sequestration*. Consensus study report. Washington, DC: The National Academies Press, 2022. 307 pp. ISBN: 978-0-309-08761-2.

[11] *NATIONAL INVENTORY REPORT 1990–2021: GREENHOUSE GAS SOURCES AND SINKS IN CANADA*. Environment and Climate Change Canada, June 2023. URL: https://www.canada.ca/en/environment-climate-change/services/climate-change/pricing-p%20ollution-how-it-will-work/output-based-pricing-system/federal-greenhouse-gas-offset-sys%20tem/emission-factors-reference-values.html#toc7.

[12] Helen Onyeaka et al. "Minimizing carbon footprint via microalgae as a biological capture". In: *Carbon Capture Science & Technology* 1 (Dec. 2021), p. 100007. ISSN: 27726568. DOI: 10.1016/j.ccst.2021.100007. URL: https://linkinghub.elsevier.com/retrieve/pii/S2772656821000075 (visited on 03/09/2025).

[13] Daniel Popa and Florin Udrea. "Towards Integrated Mid-Infrared Gas Sensors". In: *Sensors* 19.9 (May 4, 2019), p. 2076. ISSN: 1424-8220. DOI: 10.3390/s19092076. URL: https://www.mdpi.com/1424-8220/19/9/2076 (visited on 03/08/2025).

[14] Paola A. Saenz Cavazos et al. "Evaluating solid sorbents for CO2 capture: linking material properties and process efficiency via adsorption performance". In: *Frontiers in Energy Research* 11 (July 27, 2023), p. 1167043. ISSN: 2296-598X. DOI: 10.3389/fenrg.2023.1167043. URL: https://www.frontiersin.org/articles/10.3389/fenrg.2023.1167043/full (visited on 03/04/2025).

[15] Juzheng Song et al. "Moisture Swing Ion-Exchange Resin-PO_4 Sorbent for Reversible CO_2 Capture from Ambient Air". In: *Energy & Fuels* 33.7 (July 18, 2019), pp. 6562–6567. ISSN: 0887-0624, 1520-5029. DOI: 10.1021/acs.energyfuels.9b00863. URL: https://pubs.acs.org/doi/10.1021/acs.energyfuels.9b00863 (visited on 03/08/2025).

[16] *Swing adsorption*. Application report. Valmet, May 2024. URL: https://www.valmet.com/globalassets/sharepoint/imported/2730_01_01en.pdf.

[17] Tao Wang, Klaus S. Lackner, and Allen Wright. "Moisture Swing Sorbent for Carbon Dioxide Capture from Ambient Air". In: *Environmental Science & Technology* 45.15 (Aug. 1, 2011), pp. 6670–6675. ISSN: 0013-936X, 1520-5851. DOI: 10.1021/es201180v. URL: https://pubs.acs.org/doi/10.1021/es201180v (visited on 03/04/2025).

[18] J Weitkamp. "Zeolites and catalysis". In: *Solid State Ionics* 131.1 (June 1, 2000), pp. 175–188. ISSN: 01672738. DOI: 10.1016/S0167-2738(00)00632-9. URL: https://linkinghub.elsevier.com/retrieve/pii/S0167273800006329 (visited on 03/09/2025).

[19] James R. Welty, Gregory L. Rorrer, and David G. Foster. *Fundamentals of momentum, heat, and mass transfer*. 7th edition. OCLC: 1055575895. Hoboken, NJ: Wiley, 2019. ISBN: 978-1-119-72354-7.

[20] Qian Yu et al. "Enhanced biomass and CO2 sequestration of Chlorella vulgaris using a new mixotrophic cultivation method". In: *Process Biochemistry* 90 (Mar. 2020), pp. 168–176. ISSN: 13595113. DOI: 10.1016/j.procbio.2019.11.022. URL: https://linkinghub.elsevier.com/retrieve/pii/S1359511319312474 (visited on 03/09/2025).

VIII. Appendices

A. Energy Balance

TABLE II
PROTOTYPE SYSTEM COMPONENT LABELS FOR FIGURE 4

Description	Runtime per Cycle (mins)	Power per Cycle (kWh)	gCO_2 Emitted	Other Information
Dry Condition				
Blower	60	4.0e-1	12	
Lens Heater	60	1.95e-2	0.585	
Jandy 3-Way Valve	1	3.0e-4	0.009	
CO_2 Sensor	85	5.1e-5	0.00153	Continuous operation
Humid Condition				
Submersible Pump	5	3.75e-3	0.1125	
Carbonated Water Pump	2	6.8e-4	0.0204	
Motorized Ball Valve	1	1.0e-4	0.003	
Algae Cycle				
Peristaltic Pump (3)	0.4	4.8e-4	0.0144	Runs once in 13 cycles
Magnetic Stirrer	85	4.25e-2	1.275	Continuous operation
Liquid Level Sensor	85	1.4167e-6	4.25e-5	Continuous operation
Turbidity Sensor	85	1.558e-4	2.34e-4	Continuous operation
Algae Growth Light	85	1.714e-2	0.5142	Continuous operation

B. Materials Balance

TABLE III
MATERIAL COMPOSITION AND CO_2 EMISSIONS OF SYSTEM COMPONENTS

Description	Material	Material Weight (kg)	gCO_2 Emitted	Other Information
Dry Condition				
Leaf Blower	PE	1.27	2.46	
Lens Heaters	Nylon	0.122	0.809	
Jandy 3-Way Valve	Chlorinated PVC (CPVC)	1.8	6.876	
SCD41 Sensor (2)	Various	0.0074	-	Assumed to be negligible due to small size and ROHS/REACH compliance
Glass Column	Borosilicate glass	7.25	5.22	
Flanges and threaded rods	304 SS	2.875	9.387	
Vacuum Hose	ABS	0.78	2.808	
3D Printed Adapters	PLA	2	5.60	
½" Tubing	Vinyl	0.1	0.382	
½" OD Tubing	Silicone	0.15	1.133	
Metal Mesh	304 SS	0.025	0.0816	
Shelving Unit	SS + wood	22.5	53.7	
Humid Condition				
Submersible Pump	PVC	1.1	4.202	
Carbonated Water Pump	PP	0.00028	0.00049	
Mist Sprayer	PVC	0.002	0.00764	
Algae Cycle				
Peristaltic Pump (3)	PVC	0.472	1.80	
Magnetic Stirrer	Anodized Aluminum	4.2	28.308	
Turbidity Sensor (2)	Various	0.03	-	Assumed to be negligible due to small size and ROHS/REACH compliance
Grow Light	LED	0.383	1.28	Assuming 1 wafer-worth of LED and using Ontario grid data
Storage containers (5)	HDPE	2.265	5.135	
Stir bar	Alnico and PTFE	0.00925	0.111	
Bulkhead Adapter (10)	PE	0.003	0.00582	

C. Materials Carbon Tracking Data Sources

TABLE IV
AVERAGE CO_2-E OUTPUT PER KG OF MATERIAL

Material	**Average CO_2-e Output per kg (kg)**	**Sources**
Polyvinyl Chloride (PVC)	2.22	[4]
Polypropylene (PP)	1.95	[4]
Polyethylene (PE)	2.4	[4][1]
Polylactic Acid (PLA)	2.8	[1]
Acrylonitrile Butadiene Styrene (ABS)	3.46	[4]
Borosilicate Glass	0.85	[4]
Stainless Steel 304	3.29	[4]
Nylon	7.9	[4]
Silicone	2.67	[4]
Particle Board	0.200	[6]
High Density Polyethylene (HDPE)	1.9	[4]
Polytetrafluoroethylene (PTFE)	12.0	[5]
Anodized Aluminium	8.14	[4]
LED	1.28	[13][40]

D. Financial Tracking: Use of Grant Funds

TABLE V
DESCRIPTION OF ITEM CLASSIFIERS FOR GRANT FUNDING USAGE (VI)

Item Classifier	Item Description
1	For parts manufacturing
2	For air supply to column CO2 sensor
3	For air supply to column CO2 sensor
4	For controlling orbital shaker
5	Enclosure for dissolved CO2 sensor sensing unit
6	For dissolved CO2 sensor
7	Powers small electrical components
8	Parts storage
9	Electrical work/components
10	New 3D printer hotend for precision work
11	Power supply cables for components
12	Electrical work/components
13.A	Electrical work/components
13.B	”
14	Bioreactor for algae growth/testing
15.A	Hardware components for system
15.B	”
16	Parts storage/labelling
17	Column heating mechanism
18	3D printing materials
19	CO2 sensor
20	CO2 sensor (Shipping, taxes, and duties)
21.A	Hardware components for system
21.B	”
22	Hardware components for system
23.A	Electrical work/components
23.B	”
24.A	Electrical work/components
24.B	”
25	Replacement soldering irons
26	Electrical work/components
27	Hardware components for system
28	Hardware components for system
29	Hardware components for system
30	Hardware components for system
31	Column construction components
32	Brass Screw-to-Expand Inserts for Plastic

TABLE VI
GRANT FUNDING USAGE: ITEMIZED EXPENSES (CAD)

Item Classifier	Item Description	Retailer	Cost (CAD)
1	Bambu Lab P1P 3D Printer, P1P	BambuLab	706.25
2	Diaphragm Pump Kamoer KLC2-A	Amazon	59.68
3	Artshu Micro Vacuum Pump, 0.5L/min	Amazon	36.7
4	Bolsen 5pcs Reprap Stepper Driver pololu A4988	”	”
5	Custom 3D resin print	NanoPLA Studios	57
6	Custom PCBs	PCBWay	30.83
7	CR2016 Batteries 3V Lithium Cell	Amazon	10.16
8	12.9QT 4PK Clear Plastic Bins	Costco	22.58
9	Soldering Iron Kit	Amazon	45.19
10	Bambu Hotend, P1 Series	BambuLab	25.98
11	BV-Tech 12V 1A Power Supply 5 Pack	Amazon	33.89
12	Resistors, Transistors, and 12V-5V Power Converters	K-W Surplus	57.49
13.A	WGGE WG-015 Professional Wire Stripper/Wire Crimping Tool	Amazon	37.27
13.B	Striveday 18 AWG Flexible Electric Wire	”	
14	Pioreactor 20ml v1.1	Pioreactor	454.26
15.A	iMopo 300 Pcs Barbed Connectors Irrigation Fittings Kit	Amazon	54.12
15.B	Besitu 1760pcs Metric Screw Assortment	”	”
16	NIIMBOT D110 Mini Label Maker	Amazon	22.59
17	Self-Regulating Heater, 120V Ac, With Plug, 108W, 18 Feet Long	McMaster-Carr	307.49
18	ELEGOO Rapid PETG Filament 1.75mm Black 2KG	Amazon	38.41
19	T6615 SENSOR CARBON DIOXIDE 0-4V OUT	Digikey	219.11
20	T6615 SENSOR CARBON DIOXIDE 0-4V OUT	Fedex	41.14
21.A	ERHT 3D Printing Brass Nuts Threaded Inserts 360Pcs	Amazon	94.9
21.B	HOTO Electric Precision Screwdriver	”	”
22	2x Power Bars, Hose Clamps	Canadian Tire	42.42
23.A	JST PH 2.0 Connectors Pin Header and Ribbon Cable Wire Kit	Amazon	47.44
23.B	TUOFENG 24awg Wire- Flexible Silicone Wire Hook up Wires	”	”
24.A	CONN SOCKET 24-28AWG CRIMP TIN	Digikey	48.85
24.B	PLIERS ELEC NEEDLE NOSE 5.75”	”	”
25	Soldering iron	Neat Pine Store Ltd	117.77
26	FULARR 24Pcs Professional DC Connector Plug	Amazon	19.19
27	Soft Plastic Tubing for Air&Water	McMaster-Carr	52.64
28	HEROFFIX Plastic Hose Barb Fitting 1/16” to 1/8” Hose ID	Amazon	9.59
29	RATCHROLL Plastic Hose Barb Fitting 1/16”	Amazon	9.59
30	JB ClearWeld	The Home Depot	16.92
31	Square-Profile Oil-Resistant Buna-N O-Rings	McMaster-Carr	48.76
32	Brass Screw-to-Expand Inserts for Plastic	”	”
Grant Total (CAD)	2737.25	**Total Expenses (CAD)**	2768.21